

## Measurement of peroxides and related species in the 1993 North Atlantic Regional Experiment

Judith B. Weinstein-Lloyd

Chemistry and Physics Department, State University of New York at Old Westbury, Old Westbury

Peter H. Daum, Linda J. Nunnermacker, Jai H. Lee, and Lawrence I. Kleinmann

Brookhaven National Laboratory, Department of Applied Science, Environmental Chemistry Division, Upton, New York

**Abstract.** Gaseous peroxides were measured during the North Atlantic Regional Experiment (NARE) aboard the Department of Energy's Gulfstream G-1 aircraft in August 1993. Flights originated in Halifax, Nova Scotia and covered a region extending several hundred kilometers from the eastern edge of the North American continent. Total peroxide concentration was dominated by  $\text{H}_2\text{O}_2$ . Median  $\text{H}_2\text{O}_2$  concentration for all flights was 2.5 parts per billion by volume (ppbv), with the highest concentrations observed in spatially extensive layers between 250 and 1750 m above sea level. In the clean free troposphere,  $\text{H}_2\text{O}_2$  concentration correlates strongly with the product  $\text{O}_3 \cdot \text{H}_2\text{O}$ , consistent with our understanding of the formation mechanism. The median peroxide concentration was 4 ppbv in pollutant plumes, with excursions above 11 ppbv. The high concentration of  $\text{H}_2\text{O}_2$  observed, and its covariance with concentrations of anthropogenic species such as  $\text{O}_3$ ,  $\text{NO}_y$ , and aerosol particles is attributed to the aging of polluted air masses advected from the continent in stable layers.

### Introduction

Peroxides play an important role in atmospheric chemistry, both as oxidants for atmospheric  $\text{SO}_2$  [Penkett *et al.*, 1979; Calvert *et al.*, 1985] and as end products for the free radicals that participate in the formation of tropospheric ozone [Kleinman, 1986; Madronich and Calvert, 1990]. Although ambient peroxide concentrations have been measured in a number of field programs over the last decade, questions remain about sampling line losses, speciation of individual peroxides, and the importance of dry deposition in interpreting  $\text{H}_2\text{O}_2$  concentrations measured at the surface.

Pre-1989 field measurements of peroxides in air and precipitation have been summarized in two review papers [Gunz and Hoffmann, 1990; Sakugawa *et al.*, 1990]. Peroxide concentrations at the surface correlate roughly with insolation and temperature, with deposition leading to substantial decreases at night. Many features complicate the interpretation of surface measurements, including fog and rain events, local emissions, and deposition. Peroxide measurements at high altitude surface sites, while not affected by major sources, are also complicated by cloud events and boundary layer dynamics [Mohnen and Kadlec, 1989].

Heikes *et al.* [1987] measured gaseous peroxide concentrations up to 4 parts per billion by volume (ppbv) over the northeastern United States during fall 1984. Air near the surface had lower concentrations than air aloft, and vertical

profiles frequently exhibited maximum  $\text{H}_2\text{O}_2$  concentrations above cloud top. Lower concentrations (generally <1 ppbv) observed over the Carolinas in the winter of 1986 were attributed to lower rates of radical production [Barth *et al.*, 1989].  $\text{H}_2\text{O}_2$  concentrations up to 7 ppbv were observed by P. H. Daum *et al.* over Ohio during the summer of 1987. These measurements revealed a pronounced altitude dependence in peroxide concentrations with lower concentrations in the boundary layer (BL) than the free troposphere, a maximum near the top of the BL, and evidence for loss of peroxide by cloud processes. The "bulge" in peroxide concentration near the top of the BL was also observed during the same time period in the same vicinity by Boatman *et al.* [1990], and was attributed to loss by dry deposition of peroxide, reaction of its precursors with NO at lower altitudes, and lower radical production rates at higher altitudes due to decreasing water vapor concentration. Measurements in the same region during the Acid Modes study in the summer of 1988 [Tremmel *et al.*, 1993] also showed pronounced maxima in  $\text{H}_2\text{O}_2$  concentrations at the top of the BL.

Although the aircraft measurements summarized above were carried out with a dual-channel peroxide analyzer capable of distinguishing  $\text{H}_2\text{O}_2$  from total organic peroxides (ROOH), most report only  $\text{H}_2\text{O}_2$  data. Exceptions include the measurements of Barth *et al.* [1989], which showed no evidence of ROOH above the detection limit of 0.1 ppbv in winter, and of Heikes *et al.* [1987] in the fall over the northeastern United States where ROOH concentrations as large as 0.5 ppbv were reported, but were not considered to be quantitative.

The August 1993 North Atlantic Regional Experiment (NARE) was an attempt to learn more about the transport and photochemistry of ozone and ozone precursors by combining observations from measurement platforms on the ground, aloft,

and at sea. The present paper describes peroxide data obtained aboard the Department of Energy's Gulfstream G-1 aircraft, based in Halifax, Nova Scotia. A companion paper in this issue describes more fully the aircraft capabilities and instrumentation on the G-1 [Daum *et al.*, and references therein]. Synoptic patterns encountered during the mission are discussed by Berkowitz *et al.* [this issue] and Merrill and Moody [this issue]. A distinctive feature of the atmosphere over the western North Atlantic during this program was the frequent presence of a low-level inversion trapping warm air masses advected from the continent in isolated layers above the surface. The absence of substantial convective mixing allowed photochemical products to build up to high concentrations in these layers and preserved the relationship between peroxides and related species which would otherwise be lost through dry deposition.

## Experimental

### Flights

Flights of the G-1 included several west and southwesterly paths over the Bay of Fundy and Cape Sable, and several east and southeasterly paths terminating at Sable Island, approximately 250 km southeast of Halifax. Flight plans included both vertical profiles and horizontal transects, and were generally conducted in clear air, with 85% of the data collected between the hours of 1400 and 2000 UT. An overview of the G-1 flights is given in the article by Fehsenfeld *et al.* [this issue (b)].

### Instrument Description

Peroxides were determined in a two-channel continuous flow analyzer of the design of G. L. Kok and A. L. Lazrus [Kok *et al.*, 1986; Lazrus *et al.*, 1986], modified to permit analysis using Fenton chemistry [Lee *et al.*, 1990; 1994] in addition to the standard p-hydroxyphenylacetic acid/oxidase reagent in order to speciate peroxides.

A three-eighths-inch ID Teflon line, 0.75 m in length, conducted ram air to the instrument through a forward-facing inlet in the side of the plane. The instrument employs dual glass coil scrubbers to transfer gaseous peroxides into the aqueous phase, with subsequent continuous-flow derivatization to produce fluorescent products. Baselines were established several times during each flight by directing air through a Pd / alumina cartridge. Cartridge integrity was checked regularly by placing a second such cartridge upstream of the first. Signal intensity was calibrated using aqueous peroxide standards prepared daily by serial dilution of unstabilized 3% stock H<sub>2</sub>O<sub>2</sub>;

scrubbing reagent was used for the final dilution. Stock 3% peroxide was titrated against standardized permanganate before and after the measurement period. Liquid and air flow rates were calibrated several times during the measurement period. The 0 to 95% response time of the peroxide analyzer was 70 s.

The detection limit for each channel, evaluated as three times the noise level of a zero air baseline on the ground (i.e., 3σ), was 75 parts per trillion by volume (pptv). Aloft, this value increased to 0.2 ppbv. The determination of methyl hydroperoxide (MHP) from the difference between channels had a detection limit of 0.3 ppbv. The composite error in determining the concentration of peroxide standards and liquid and air flow rates was 3.5%.

SO<sub>2</sub> interference was evaluated by monitoring the signal from an aqueous H<sub>2</sub>O<sub>2</sub> standard in the presence of gas phase SO<sub>2</sub> of known concentration. No change in response was observed for SO<sub>2</sub> concentrations below 150 ppbv, well above the SO<sub>2</sub> concentrations encountered in the region.

### Speciation of Peroxides

Analysis of gaseous peroxides in urban environments by the recently developed HPLC method has shown only H<sub>2</sub>O<sub>2</sub>, methyl hydroperoxide (CH<sub>3</sub>OOH or MHP) and hydroxymethyl hydroperoxide (HOCH<sub>2</sub>OOH or HMHP) to be present in significant concentrations in ambient air [Hellpointner and Gáb, 1989; Hewitt and Kok, 1991; Fels and Junkermann, 1994]. A continuous-flow instrument capable of analyzing for these three species in real time has been developed [Lee *et al.*, 1990; 1994] but is not yet available for aircraft deployment. Therefore we analyzed for two of the three peroxides using the standard dual channel instrument. Two factors guided our selection of the two peroxides to monitor: (1) HMHP is believed to be a product of the ozonolysis of alkenes [Simonaitis *et al.*, 1991; Hewitt and Kok, 1991], and its concentration is expected to be greatest near the surface [Enders *et al.*, 1992]; and (2) ground measurements at the start of the program at Yarmouth, Nova Scotia indicated negligible concentrations of HMHP [J. B. Weinstein-Lloyd *et al.*, Peroxide Measurements in Yarmouth, NS, during the 1993 NARE summer intensive, manuscript to be submitted to *J. Geophys. Res.*, 1996]. Therefore the dual-channel instrument was configured to yield measurements of H<sub>2</sub>O<sub>2</sub> and MHP.

Reagents employed in the dual channel system are summarized in Table 1. In channel A, the horseradish peroxidase-catalyzed reaction between peroxide and p-hydroxyphenylacetic acid (pOHPAA/HRP) produces a fluorescent dimer; and signal intensity is increased by raising pH. In Channel B, Fenton reagent, consisting of a mixture of Fe(II) and benzoic acid (FeBA) produces fluorescent hydroxy-

Table 1. Reagents for Peroxide Analyzer

CH	Scrubbing Solution*	Fluorescence Reagent*	Enhancing Reagent*	Species Detected
A	1 mM phosphate buffer, pH 9; 1 mM HCHO	3.5 mM pOHPAA; HRP 2 units/mL; pH 8.5 TRIS buffer	0.05 N NaOH	H <sub>2</sub> O <sub>2</sub> + MHP
B	1 mM phosphate buffer, pH 9; 1 mM HCHO	0.8 mM FeSO <sub>4</sub> ; 2 mM benzoic acid; pH 1.9 H <sub>2</sub> SO <sub>4</sub>	6 mM Al(NO <sub>3</sub> ) <sub>3</sub> ; 10 mM acetate buffer, pH 3.8	H <sub>2</sub> O <sub>2</sub>

\* all solutions prepared with conductivity grade water

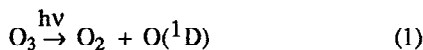
benzoic acid upon reaction with  $\text{H}_2\text{O}_2$ ; fluorescence intensity is enhanced in this channel by  $\text{Al(III)}$  complexation. HMHP rapidly hydrolyzes to produce  $\text{H}_2\text{O}_2$  in the high pH scrubbing solution in both channels, causing the aqueous stream meeting fluorescence reagents to be a solution of  $\text{H}_2\text{O}_2$  and MHP only [Marklund, 1971]. pOHPAA/HRP reacts with all peroxides with equal efficiency, while FeBA is specific for  $\text{H}_2\text{O}_2$ . Therefore channel A provides a measure of total peroxide, and channel B provides only  $\text{H}_2\text{O}_2$ . MHP is reported in this work as the difference between channels A and B after correcting for the collection efficiency of MHP, taking into account a recent correction to its published Henry's law constant [Lind and Kok, 1994; Lind et al., 1986]. Two caveats should be noted when viewing the peroxide data. As discussed above, measurements at the program's start indicated negligible surface concentrations of HMHP, and we report  $\text{H}_2\text{O}_2$  as the signal from channel B in this work. However, surface measurements may not be representative of conditions aloft, and as ambient HMHP (or other soluble, hydrolyzable peroxides) would have been collected and converted to  $\text{H}_2\text{O}_2$  in both channels, concentrations of  $\text{H}_2\text{O}_2$  reported here should be viewed as an upper limit. In addition, any water soluble higher peroxide that did not hydrolyze, would produce a fluorescent dimer in the pOHPAA channel, but would not produce OHBA in the FeBA channel [Kolthoff and Medalia, 1951]. Thus MHP concentrations reported here actually represent the sum of all nonhydrolyzable peroxides collected.

To demonstrate that MHP does not give a signal in the Fenton channel, we analyzed mixtures of  $\text{H}_2\text{O}_2$  and MHP produced by cobalt-60  $\gamma$ -radiolysis of aqueous solutions of  $\text{CH}_3\text{I}$  [Shankar et al., 1969]. Irradiated samples were analyzed simultaneously in the dual-channel instrument and by high performance liquid chromatography with post-column pOHPAA/HRP derivatization; the percentage MHP determined agreed to within 15%.

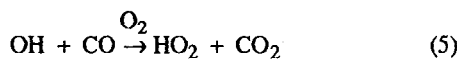
## Results and Discussion

Peroxides are formed by the photochemical mechanism summarized in reactions (1) - (12) below.

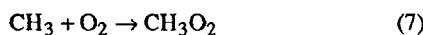
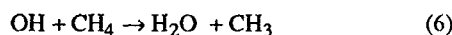
### Initiation



### Formation of $\text{HO}_2$ Radicals



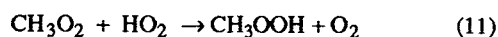
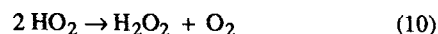
### Formation of $\text{RO}_2$ Radicals



### Reaction with NO



### Radical Termination Reactions



$\text{H}_2\text{O}_2$  is formed principally by the disproportionation of  $\text{HO}_2$  radicals, reaction (10). In polluted environments, reaction of  $\text{HO}_2$  with NO, reaction (8), competes with disproportionation, and the subsequent photolysis of  $\text{NO}_2$  is a major source of tropospheric ozone. The abundance of atmospheric  $\text{CH}_4$  implies that methylperoxyl radicals ( $\text{CH}_3\text{O}_2$ ) will be produced by reactions (1) and (2), followed by (6) and (7). Reaction (11) should then produce measurable quantities of MHP, which together with other peroxides can oxidize  $\text{SO}_2$  and increase the acidity of cloud water [Lind et al., 1987]. The mechanism summarized above suggests that the eventual sink for photochemically produced free radicals must be either peroxide formation or  $\text{NO}_x$  oxidation products such as  $\text{HNO}_3$  and peroxyacetyl nitrate (PAN).

### General Observations

Concentrations of hydrogen peroxide varied from the detection limit to over 11 ppbv, with the highest concentrations observed in transported plumes of anthropogenic pollution at altitudes near 1 km. These plumes, containing high concentrations of  $\text{O}_3$ ,  $\text{NO}_y$ , and related species began to be observed in the region after August 20. The early portion of the field program was characterized by light winds and anticyclonic flow, with background concentrations of photochemically related species.

A histogram of the complete data set, shown in Figure 1, exhibits a median  $\text{H}_2\text{O}_2$  concentration of 2.5 ppbv. Median concentrations were higher in the boundary layer (2.7 ppbv) than in the free troposphere (2.2 ppbv), where boundary layer air is defined as air with dew point greater than zero. The composite vertical distribution of  $\text{H}_2\text{O}_2$ , illustrated in Figure 2, shows median peroxide concentrations between 1 and 3 ppbv. The gradual decrease in peroxide concentration with increasing altitude above the boundary layer presumably arises from decreasing OH production consistent with decreasing water vapor concentration. Deposition may contribute to the slight decrease in median concentrations observed near the surface, but episodes of high  $\text{H}_2\text{O}_2$  concentration are evident at altitudes between 250 and 1750 m. Simultaneous measurements of other

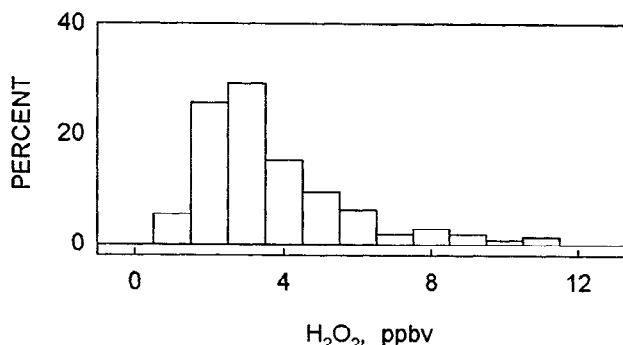
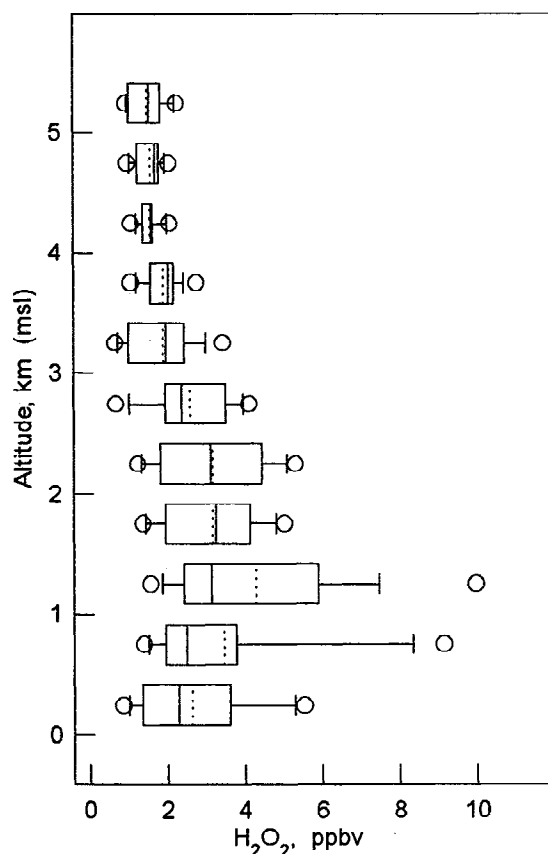


Figure 1. Frequency distribution of  $\text{H}_2\text{O}_2$  measurements, all data.



**Figure 2.** Composite vertical profile of peroxide measurements for the entire program. Box encloses upper and lower quartiles, with the median and mean displayed as solid and dashed lines, respectively. Extension lines enclose the 10th and 90th percentiles and circles represent outliers.

trace gas species suggest that these layers of high, variable  $\text{H}_2\text{O}_2$  concentration are associated with plumes of anthropogenic origin [see Daum *et al.*, this issue].

MHP was detected on only 3 of the 14 flights, on August 17, 20 and 31; median concentrations of 0.45, 0.73, and 0.54 ppbv, respectively, were observed. No trends were apparent in the MHP data.

### Individual Flights

Prior to August 20, flights sampled generally clean background air. On August 24, southwesterly winds began to move into the region, but it was several days before well-defined flow brought significant concentrations of pollutants from the continent. Several plumes were observed on flights from August 25 through August 31. These air masses were characterized by high concentrations of particles and  $\text{NO}_y$ , and most were well aged, as evidenced by the high levels of ozone and the large fractional conversion of  $\text{NO}_x$  to  $\text{HNO}_3$ . These regions also exhibited high peroxide concentrations. The photochemical mechanism for peroxide formation suggests that fresh air masses with high  $\text{NO}_x$  should be characterized by high  $\text{O}_3$  from  $\text{NO}_2$  photolysis and by low  $\text{H}_2\text{O}_2$  concentration because of the competition for  $\text{HO}_2$  radicals. The inverse relationship between  $\text{H}_2\text{O}_2$  and  $\text{NO}_y$  and between  $\text{H}_2\text{O}_2$  and  $\text{O}_3$  is not expected to persist after the air mass leaves the source region as subsequent photochemistry produces additional  $\text{H}_2\text{O}_2$  in  $\text{NO}_x$ -depleted air

Our measurements show a variety of relationships between  $\text{H}_2\text{O}_2$ ,  $\text{NO}_y$ , and  $\text{O}_3$  in polluted air masses. Several case studies are examined below to illustrate the range of behavior observed.

**August 18.** Background air was sampled on the August 18 flight between Halifax and Sable Island. This flight was typical of the early portion of the measurement program, with concentrations of  $\text{NO}_y$  below 1 ppbv, and accumulation mode aerosol particle number concentration (measured by PMS ASASP) generally below  $200 \text{ cm}^{-3}$ . A layer of very dry air (dew point  $-20^\circ$  to  $-30^\circ\text{C}$ ) was traversed on the forward leg at an altitude of 1500 m and during the return leg at 2150 m (regions A and B in Figure 3). Despite ozone concentrations in excess of 50 ppbv in this region,  $\text{H}_2\text{O}_2$  remained below 2 ppbv, presumably due to low water vapor concentration.

The 2150-m transect crossed a sharp boundary between air masses at 1800 UT (point C in Figure 3), where dew point changed from  $-30^\circ$  to  $0^\circ\text{C}$ , corresponding to a 20-fold increase in water vapor mixing ratio. At the same time,  $\text{H}_2\text{O}_2$  concentration increased by a factor of 3, from 1 to 3 ppbv, and ozone concentration dropped from 57 to 32 ppbv. The high-ozone air mass may have descended from higher altitudes with peroxide formation inhibited by dryness. Alternatively, it may be photochemically aged air that has lost  $\text{H}_2\text{O}_2$  and  $\text{NO}_x$  oxidation products through wet deposition.

**August 27.** The August 27 flight consisted of a profile over Halifax, followed by a flight to the southwest at an altitude of 1050 m to a point 150 km due east of Boston, another profile to 3800 m, and a return to the southern tip of Nova Scotia at 145 m. The initial flight leg (region A of Figure 4) was characterized by concentrations of  $\text{O}_3$  around 50 ppbv,  $\text{H}_2\text{O}_2$  around 5 ppbv and  $\text{NO}_y$  below 2 ppbv. A low-lying layer of pollutants was encountered during a descent to an altitude of 145 m and the return flight (region B in Figure 4) was made in this layer. Ozone concentration exceeded 100 ppbv,  $\text{NO}_y$  reached nearly 20 ppbv, and  $\text{H}_2\text{O}_2$  concentration decreased to approximately 1 ppbv. The highly layered structure, evident in the much lower concentrations of  $\text{NO}_y$  and  $\text{O}_3$  on the forward transect, is illustrated in Figure 5 by the vertical distributions of  $\text{H}_2\text{O}_2$ ,  $\text{O}_3$  and  $\text{NO}_y$  obtained during a sounding at  $42^\circ\text{N}$ ,  $69^\circ\text{W}$ , point C in Figure 4.

Figure 6 shows that the concentration of  $\text{H}_2\text{O}_2$  varied inversely with that of  $\text{NO}_x$  ( $r^2 = 0.97$ ) during the flight through the low-lying layer, as one would expect from the competition between reactions (8) and (10) if this were a fresh air mass.  $\text{H}_2\text{O}_2$  was also strongly anticorrelated with  $\text{O}_3$  in the plume ( $r^2 = 0.93$ ), consistent with the production of  $\text{O}_3$  from  $\text{NO}_2$  photolysis. Back trajectories place this air mass over the continent only 6 hours prior to our measurements, and  $\text{NO}_x$  contributes nearly 2 ppbv to a peak  $\text{NO}_y$  concentration of 16 ppbv.

**August 28.** Elevated concentrations of pollutants were also evident on August 28 on a flight south and east of Halifax. Concentrations of  $\text{H}_2\text{O}_2$  and related species are illustrated for the entire flight in Figure 7. The flight path included a south-bound leg at an altitude of 630 m and a return at 1240 m, with two soundings to probe the vertical boundaries of the layer. The second of these profiles, conducted at point A in Figure 7, passed through a moist air mass trapped between two inversions. Figure 8 shows that the layer is  $\sim 1$  km thick, lying between 500 and 1500 m. In the trapped layer, peak concentrations of  $\text{H}_2\text{O}_2$  and  $\text{NO}_y$  reached 9 ppbv, and  $\text{O}_3$  reached 120 ppbv. Even higher concentrations were observed during the 630 m transect (region B of Figure 7), with ozone peaking at  $\sim 145$ ,  $\text{NO}_y$  at  $\sim 17$ ,

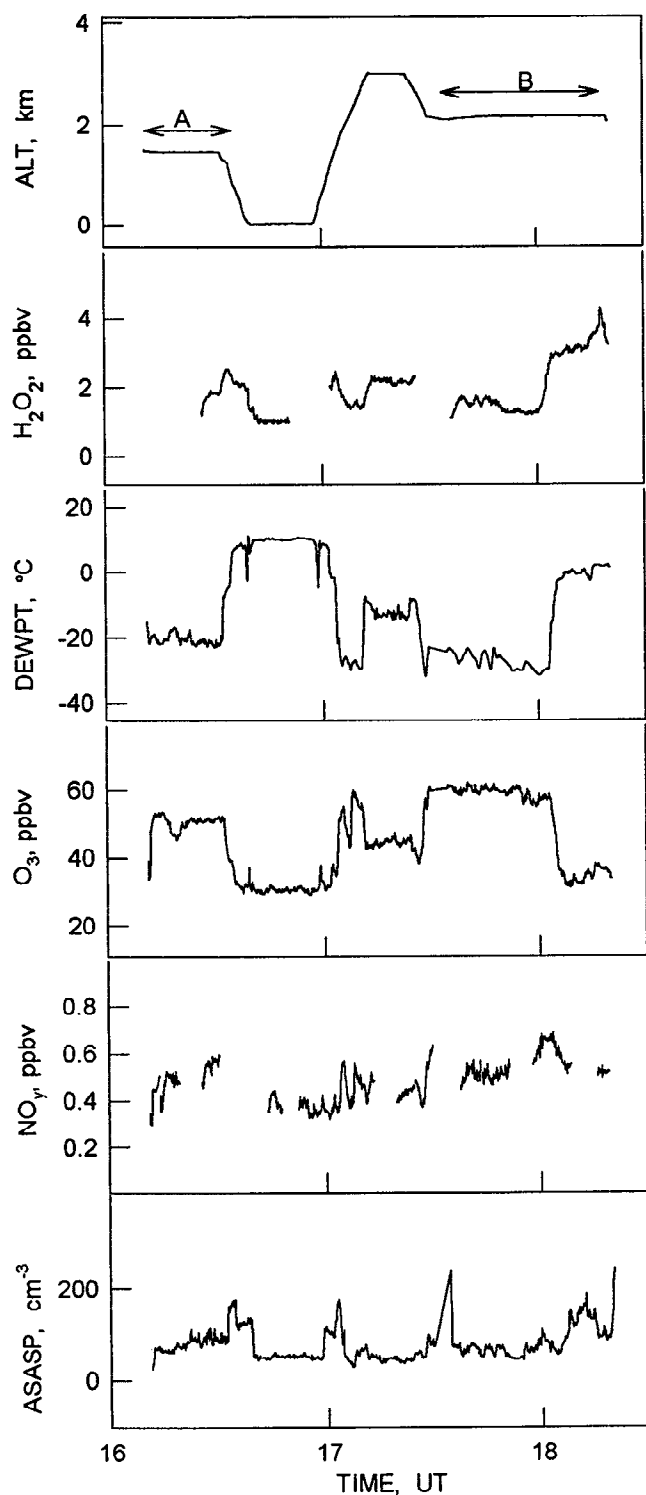


**Figure 3.** Concentrations of selected species on August 18 as a function of time. Horizontal transects, indicated as regions A and B, are described in the text.

and  $\text{H}_2\text{O}_2$  at  $\sim 10$  ppbv. Pollutant concentrations were also elevated during the return trip at 1240 m (region C in Figure 7), though not as high as on the lower altitude portion. A horizontal boundary was crossed during a short eastward leg at the same altitude (point D of Figure 4), with an abrupt decrease of roughly 33% in the concentrations of  $\text{H}_2\text{O}_2$ ,  $\text{O}_3$ , and  $\text{NO}_y$ .

The dependence of  $\text{H}_2\text{O}_2$  concentration on  $\text{O}_3$  and  $\text{NO}_y$  is very different in different regions of this plume. There is an

inverse relationship between the concentrations of  $\text{H}_2\text{O}_2$  and  $\text{O}_3$  ( $r^2 = 0.76$ ) and between  $\text{H}_2\text{O}_2$  and  $\text{NO}_y$  ( $r^2 = 0.86$ ) observed during the 630-m transect (region B in Figure 7), as on August 27th. However, on the 1240-m transect (region C, Figure 7), there is a positive correlation between  $\text{H}_2\text{O}_2$  and  $\text{O}_3$  ( $r^2 = 0.89$ )

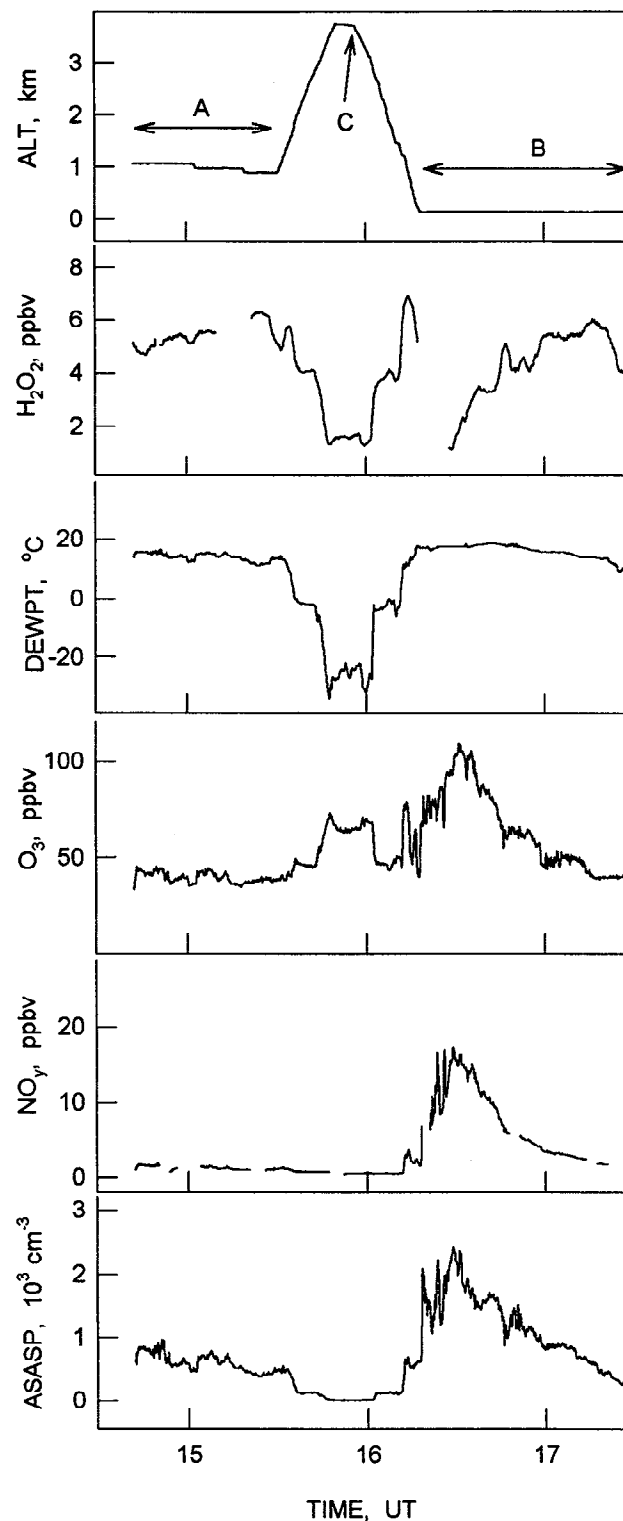


**Figure 4.** Concentrations of selected species on August 27 as a function of time. The horizontal transect indicated as region A and the plume encountered in the region shown as B are described in the text.

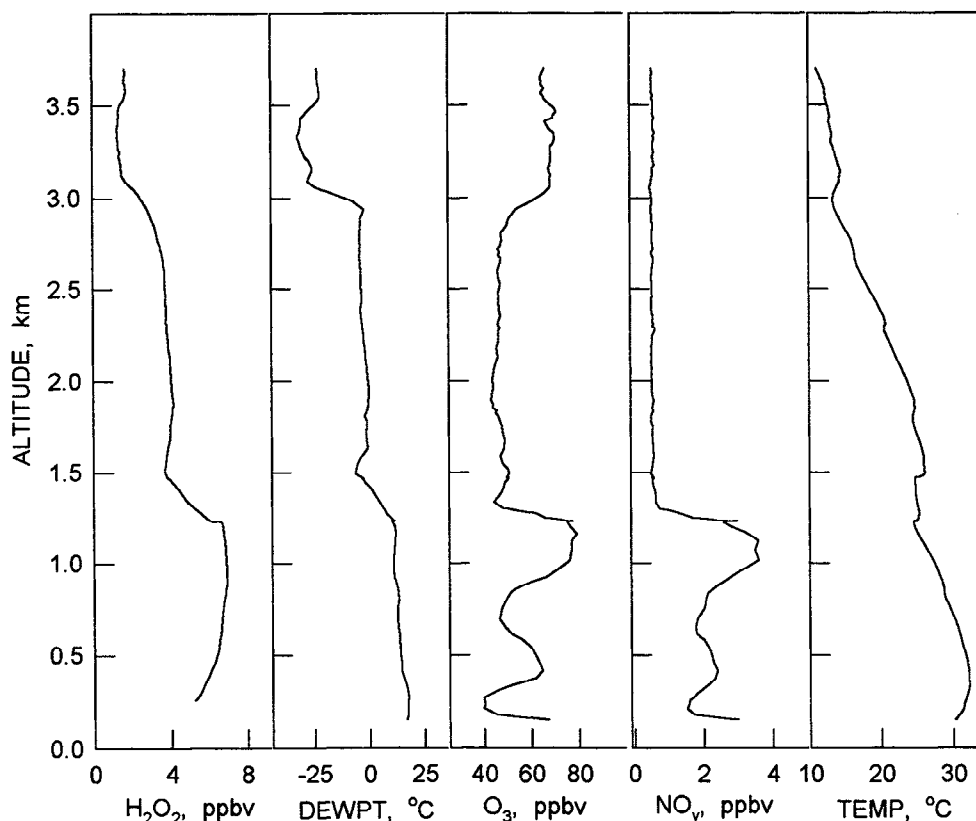


Figure 5. Vertical distribution of selected species on August 27 illustrating pollutant layer traversed during sounding at point C in Figure 4.

and between  $\text{H}_2\text{O}_2$  and  $\text{NO}_y$  ( $r^2 = 0.90$ ). In contrast to the plume sampled on August 27, this plume is estimated to have taken ~72 hours to reach Nova Scotia from the source region, consistent with the observation that virtually all of the  $\text{NO}_x$  had been depleted.

**August 31.** Elevated concentrations of  $\text{H}_2\text{O}_2$ ,  $\text{O}_3$ , and  $\text{NO}_y$  were again observed on the August 31 flight. The first portion of the flight, passing over land to the coast of Maine at an altitude of ~1 km, exhibited fairly low concentrations of these species (region A in Figure 9). On the southward leg to 42.5°N, 68°W (region B in Figure 9), the concentration of  $\text{H}_2\text{O}_2$  rose to ~8,  $\text{O}_3$  to ~70, and  $\text{NO}_y$  to ~4 ppbv. A sounding at this location (point C in Figure 9) revealed the presence of a layer containing high concentrations of  $\text{NO}_y$  and aerosol particles at ~1500 m. The vertical profile for this sounding, illustrated in Figure 10, shows the layers to be somewhat more diffuse than on earlier days, due perhaps to the absence of a well-defined inversion above the surface. The high- $\text{NO}_y$  air mass sampled during the return leg, region D in Figure 9, is well aged, with virtually no  $\text{NO}_x$  remaining, as shown by the lower trace in the  $\text{NO}_y$  panel in Figure 9. In contrast to the well-aged plumes observed on August 27 and 28, this air mass shows no correlation between  $\text{H}_2\text{O}_2$  and  $\text{NO}_y$  or between  $\text{H}_2\text{O}_2$  and  $\text{O}_3$ .

#### Peroxide Relationships in the Free Troposphere

In the free troposphere, where  $\text{NO}_x$  concentrations are low and peroxides are the principal radical sink, peroxide formation is expected to depend on ozone photolysis rate and the concentrations of ozone and water vapor [Kleinman, 1986; 1991]. Figure 11 shows that the concentration of  $\text{H}_2\text{O}_2$  correlates strongly ( $r^2 = 0.80$ ) with the product of concentrations of  $\text{H}_2\text{O}$

and  $\text{O}_3$  for altitudes above 1500 m. Over 90% of the points in this high-altitude subset exhibit  $\text{NO}_y$  concentrations below 1.5 ppbv, and the correlation is lost when low altitude, higher  $\text{NO}_y$  data is included.

The regression line in Figure 11 is what we expect based on a simple steady state model in which the concentration of  $\text{H}_2\text{O}_2$  is linearly related to the production rate of free radicals, which in turn is approximately proportional to the product of water vapor and ozone. Figure 11 indicates that this model can account for most of the variance in the low  $\text{NO}_y$  data subset. However, a change in the relation between  $\text{H}_2\text{O}_2$  and  $\text{O}_3 \cdot \text{H}_2\text{O}$  is evident at low radical production rates, that is, values of  $\text{O}_3 \cdot \text{H}_2\text{O}$  below 100 ppm<sup>2</sup>. This may be due to the dependence of  $\text{H}_2\text{O}_2$  lifetime on OH concentration, together with the dependence of OH concentration on radical production rate. Detailed photochemical model calculations are needed to investigate this possibility.

#### Correlation Between $\text{O}_3$ and $(\text{NO}_x + 2\text{H}_2\text{O}_2)$

The relationship between  $\text{H}_2\text{O}_2$ ,  $\text{O}_3$  and  $\text{NO}_y$  for plume data can be understood in terms of a correlation noted by Sillman [1995] in his model calculations of  $\text{O}_3$ - $\text{NO}_x$ -ROG sensitivity. Sillman observed that  $\text{O}_3$  concentration correlated with the sum of  $\text{H}_2\text{O}_2$  and  $\text{NO}_x$  oxidation products, that is,  $\text{NO}_y$ - $\text{NO}_x$  or  $\text{NO}_z$ ; the correlation was strongest over water where model deposition rates were low. This relationship emphasizes  $\text{O}_3$  as radical source, and the quantity  $\text{NO}_x + 2\text{H}_2\text{O}_2$  as radical sink, allowing for the 2:1 stoichiometry in forming  $\text{H}_2\text{O}_2$  from  $\text{HO}_2$  radicals. It applies whether the dominant radical sink is peroxide or  $\text{HNO}_3$  formation, and whether the air mass is fresh or aged.

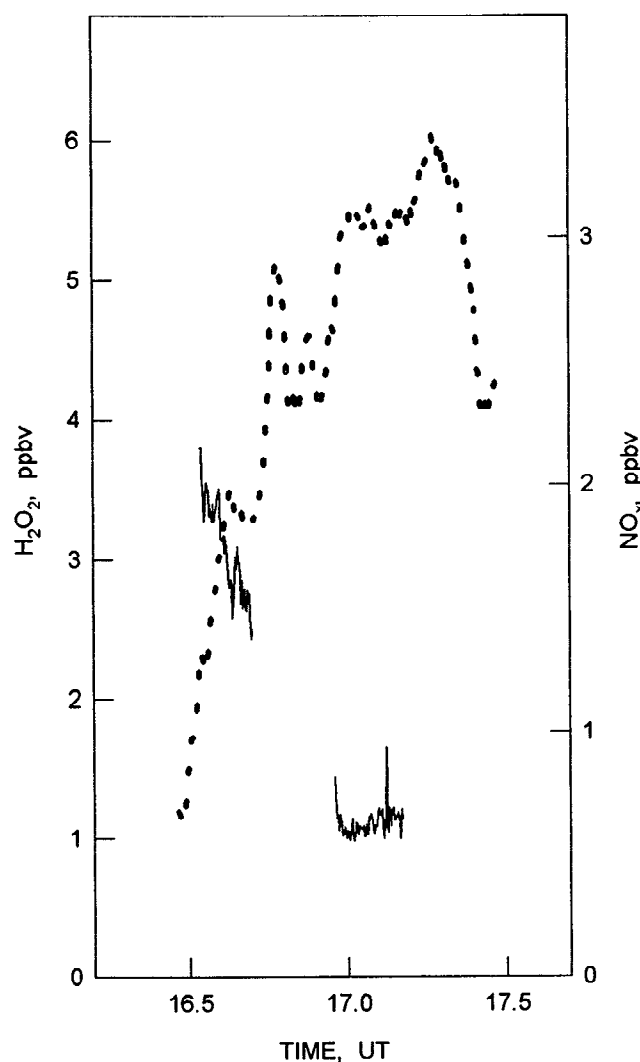


**Figure 6.** Inverse relation between  $\text{H}_2\text{O}_2$  (dotted line) and  $\text{NO}_x$  (solid line) on August 27 during a plume transect at 145 m at 16.4 UT.

Although individual subsets of the NARE data exhibit very different relationships among  $\text{H}_2\text{O}_2$ ,  $\text{O}_3$ , and  $\text{NO}_y$ , as described in the case studies above, the complete data set exhibits a linear correlation ( $r^2 = 0.73$ ) between  $\text{O}_3$  and  $\text{NO}_2 + 2\text{H}_2\text{O}_2$ , as illustrated by *Daum et al.* [this issue]. The lack of vertical mixing and wet deposition prevailing during this period facilitated the observation of this relationship.

## Summary

Peroxide concentrations varying from the detection limit to over 11 ppbv were observed over the eastern North Atlantic in the summer of 1993, with the highest concentrations occurring in well-defined layers above the surface inversion. The composite data set exhibits only a shallow concentration maximum near the top of the boundary layer ( $\sim 2$  km), in contrast to other aircraft studies conducted over the continent where the boundary layer is well mixed [*Heikes et al.*, 1987; *Boatman et al.*, 1990; *Tremmel et al.*, 1993]. Plumes of high  $\text{H}_2\text{O}_2$  concentration frequently were found in well-aged air masses advected from the continent along with high concentrations of anthropogenic pollutants. The observation of high  $\text{H}_2\text{O}_2$  concen-

trations above the surface inversion underscores the difficulty in interpreting surface measurements of photochemically important species.

Total peroxide was dominated by  $\text{H}_2\text{O}_2$ , with MHP concentrations near 0.5 ppbv observed on only 3 of 14 flights. The absence of MHP is interesting in light of the high  $\text{H}_2\text{O}_2$  concentrations observed in plumes, and merits further investigation.

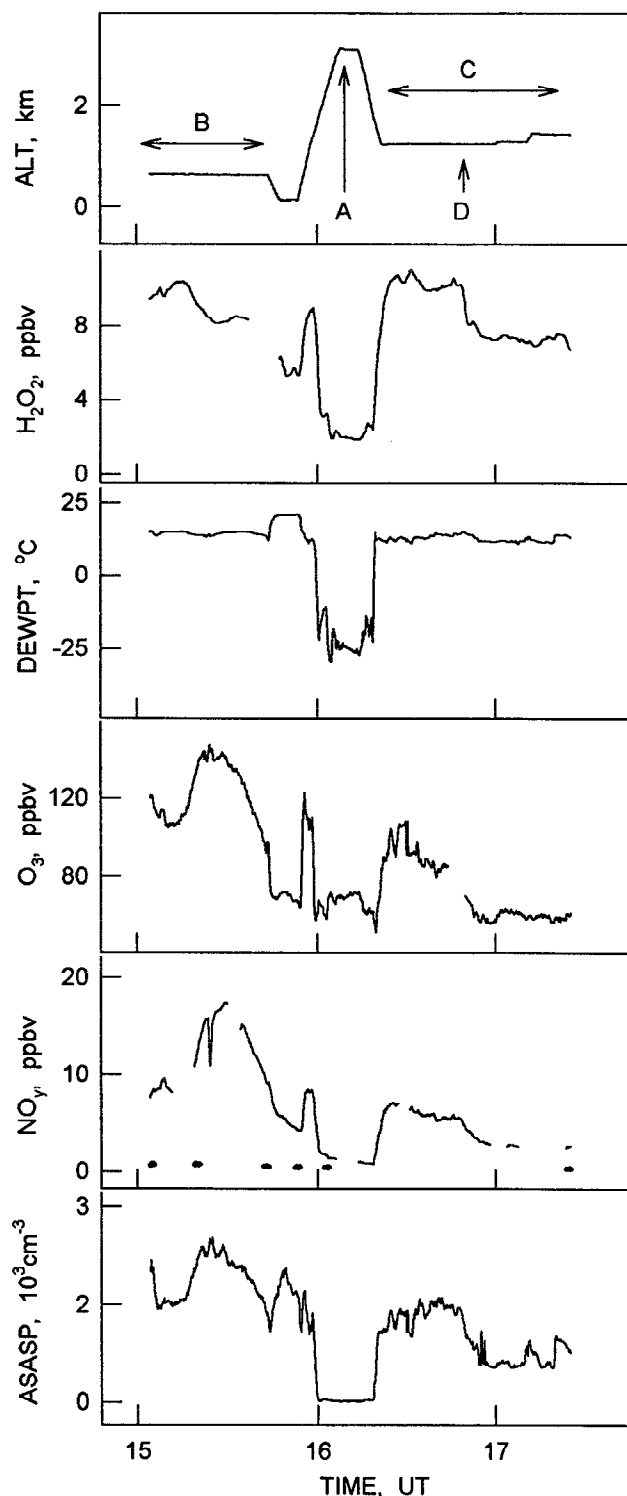


**Figure 7.** Concentrations of selected species on August 28 as a function of time. Horizontal transects, indicated by regions B and C are described in the text. Dashed line in the  $\text{NO}_y$  panel represents  $\text{NO}_x$ .

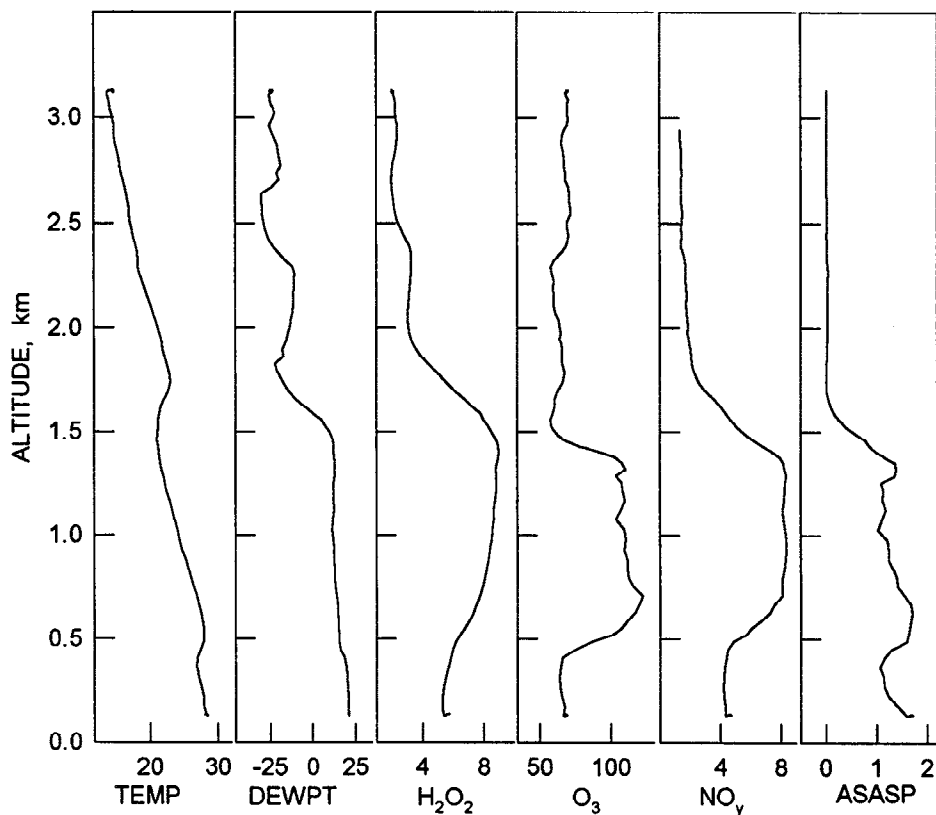


**Figure 8.** Vertical distribution of selected species at August 28 illustrating pollutant layer traversed during sounding at point A in Figure 7. Units are the same as in Figure 7.

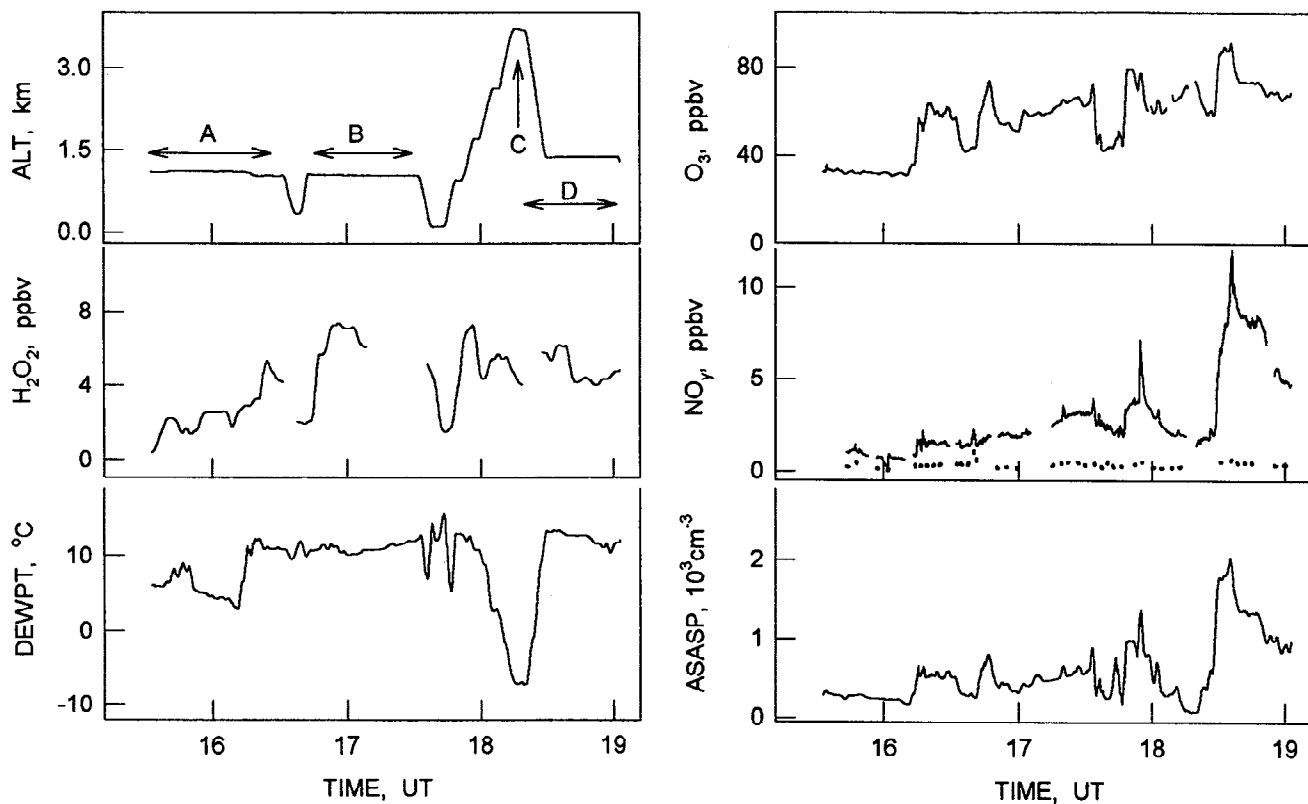


**Figure 9.** Concentrations of selected species on August 31 as a function of time. Horizontal transects, indicated by regions A, B, and D are described in the text. Dashed line in the  $NO_y$  panel represents  $NO_x$ .



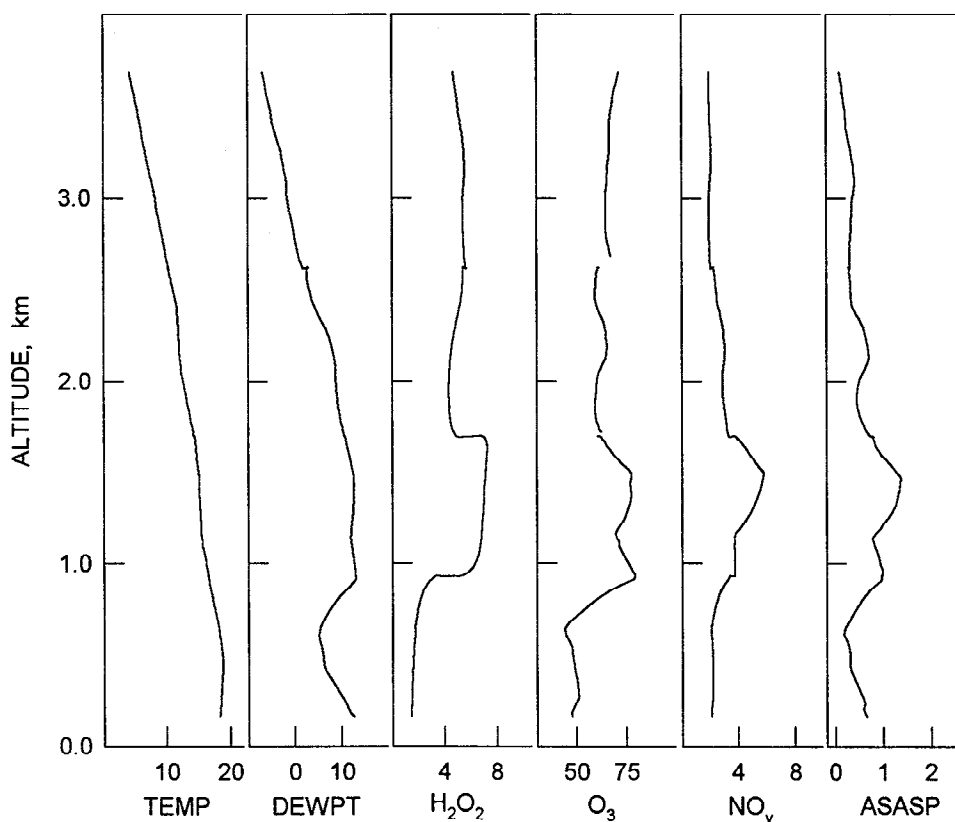


**Figure 10.** Vertical distribution of selected species on August 31 illustrating pollutant layer traversed during sounding at point C in Figure 11. Units are the same as in Figure 9.

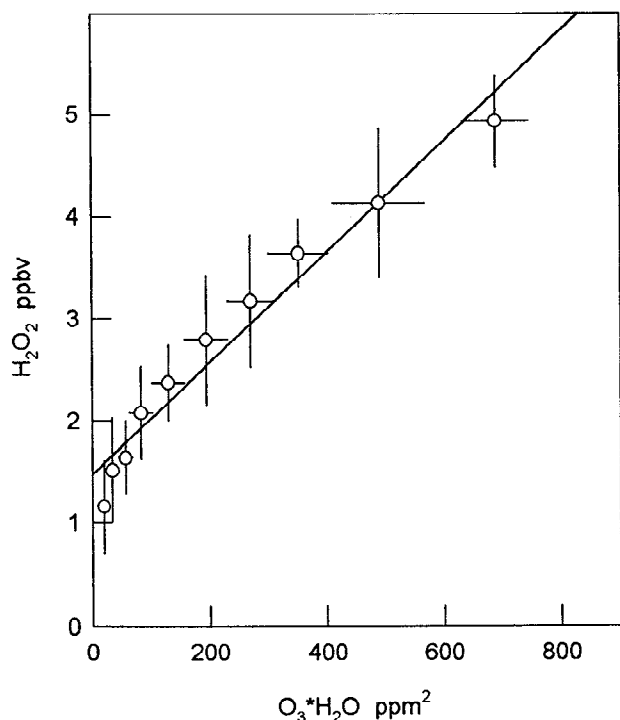


**Figure 11.** Correlation between  $\text{H}_2\text{O}_2$  and the product of  $\text{O}_3$  and  $\text{H}_2\text{O}$  in the free troposphere, i.e. data with  $[\text{NO}_y] < 1.5$  ppbv. Data were sorted in order of increasing  $x$  value, and collected in 10 groups of equal size; the mean is indicated by a circle and lines show the range of  $x$  and  $y$  values for each group. A linear regression through the means is included.

A strong correlation between  $\text{H}_2\text{O}_2$  concentration and the product  $\text{H}_2\text{O} \cdot \text{O}_3$  was observed in "clean" free tropospheric air, that is, air masses with  $\text{NO}_y$  concentrations below 1.5 ppbv, confirming our understanding of the formation mechanism for  $\text{H}_2\text{O}_2$  under conditions of low  $\text{NO}_x$  and minimal depositional losses.

In pollutant plumes, the relationship between  $\text{H}_2\text{O}_2$  concentration and that of other species is complicated. These regions are characterized by high concentrations of  $\text{NO}_y$ ,  $\text{O}_3$  and aerosol particles, indicating that they have been subjected to substantial photochemistry at the source region and during transport to Nova Scotia. Peroxide concentrations are also high in these plumes. Individual horizontal transects within polluted layers exhibit  $\text{H}_2\text{O}_2$  concentration with the inverse dependence on  $\text{O}_3$ , and  $\text{NO}_x$  characteristic of fresh air masses, or the direct relationship expected in  $\text{NO}_x$ -depleted air. Detailed model calculations are required to unravel these different behaviors.

**Acknowledgments.** We are grateful for the assistance of D. Leahy, K. Busness, J. Musa, B. Kaufman, and M. Litchy. This work was supported by NSF-RUI (ATM-9112698) and DOE (DE-FG02-91ER61206) grants to J. Weinstein-Lloyd and was performed under the auspices of the U.S. Department of Energy, under contracts DE-AC02-76CH00016.

## References

- Barth, M.C., D.A. Hegg, P.V. Hobbs, J.G. Walega, G.L. Kok, B.G. Heikes, and A.L. Lazrus, Measurement of atmospheric gas-phase and aqueous-phase hydrogen peroxide concentrations in winter on the east coast of the United States, *Tellus*, **41B**, 61-69, 1989.

- Berkowitz, C.M., P.H. Daum, C. Spicer, and K. Busness, Synoptic patterns associated with the flux of excess ozone to the western North Atlantic, *J. Geophys. Res.*, *this issue*.
- Boatman, J.F., N. Laulainen, J. Ray, C.V. Valin, L. Gunter, R. Lee, D. Lueken, and K. Busness, Acid precursor concentrations above the northeastern United States during summer 1987: Three case studies, *J. Geophys. Res.*, *95*, 11,831-11,845, 1990.
- Calvert, J.G., A. Lazrus, G.L. Kok, B. Heikes, J. Walega, J. Lind, and C.A. Cantrell, Chemical mechanisms of acid generation in the troposphere, *Nature*, *317*, 27-35, 1985.
- Daum, P.H., L.I. Kleinman, A.J. Hills, A.L. Lazrus, A.C.D. Leslic, K. Busness, and J. Boatman, Measurement and interpretation of concentrations of  $\text{H}_2\text{O}_2$  and related species in the upper Midwest during summer, *J. Geophys. Res.*, *95*, 9857-9871, 1990.
- Daum, P.H., L.I. Kleinman, L. Newman, W. Luke, J.B. Weinstein-Lloyd, C.M. Berkowitz, and K. Busness, Chemical and physical properties of plumes of anthropogenic pollutants transported over the North Atlantic during NARE, *J. Geophys. Res.*, *this issue*, 1995.
- Enders, G., et al., Biosphere/atmosphere interactions: Integrated research in a European coniferous forest ecosystem, *Atmos. Environ.*, *26A*, 171-189, 1992.
- Fehsenfeld, F.C., S. Penkett, M. Trainer, and D.D. Parish, NARE 1993 summer intensive: Foreward, *J. Geophys. Res.*, *this issue*.
- Fehsenfeld, F.C., P. H. Daum, W. R. Leatch, and G. Hubler, Transport and processing of  $\text{O}_3$  and  $\text{O}_3$  precursors over the North Atlantic: An overview of the 1993 NARE intensive, *J. Geophys. Res.*, *this issue*.
- Fels, M., and W. Junkerman, The occurrence of organic peroxides in air at a mountain site, *Geophys. Res. Lett.*, *21*, 341-344, 1994.
- Gunz, D., and M.R. Hoffmann, Atmospheric chemistry of peroxides: A review, *Atmos. Environ.*, *24*, 1601-1633, 1990.
- Heikes, B.G., G.L. Kok, J.G. Walega, and A.L. Lazrus,  $\text{H}_2\text{O}_2$ ,  $\text{O}_3$  and  $\text{SO}_2$  measurements in the lower troposphere over the eastern United States during Fall, *J. Geophys. Res.*, *92*, 915-931, 1987.
- Hellpointner, E., and S. Gäb, Detection of methyl, hydroxymethyl and hydroxethyl hydroperoxides in air and precipitation, *Nature*, *337*, 631-634, 1989.
- Hewitt, C.N., and G.L. Kok, Formation and occurrence of organic peroxides in the troposphere: Laboratory and field observations, *J. Atmos. Chem.*, *12*, 181-194, 1991.
- Kleinman, L.I., Photochemical formation of peroxides in the boundary layer, *J. Geophys. Res.*, *91*, 10889-10904, 1986.
- Kleinman, L.I., Seasonal dependence of boundary layer peroxide concentration: The low and high  $\text{NO}_x$  regimes, *J. Geophys. Res.*, *96*, 20721-20733, 1991.
- Kok, G.L., K. Thompson, A.L. Lazrus, and S.E. McLaren, Derivatization technique for the determination of peroxides in precipitation, *Anal. Chem.*, *58*, 1182-1194, 1986.
- Kolthoff, I.M., and A.I. Medalia, Determination of organic peroxides by reaction with ferrous iron, *Anal. Chem.*, *23*, 595-603, 1951.
- Lazrus, A.L., G.L. Kok, J.A. Lind, S.N. Gitlin, B.G. Heikes, and R.E. Shetter, Automated fluorometric method for hydrogen peroxide in atmospheric precipitation, *Anal. Chem.*, *58*, 594-597, 1986.
- Lee, J.H., I.N. Tang, and J.B. Weinstein-Lloyd, Non-enzymatic method for the determination of hydrogen peroxide in atmospheric samples, *Anal. Chem.*, *62*, 2381-2384, 1990.
- Lee, J.H., I.N. Tang, J.B. Weinstein-Lloyd, and E.B. Halper, Improved non-enzymatic method for determination of gas-phase peroxides, *Environ. Sci. Technol.*, *28*, 1180-1185, 1994.
- Lind, J.A., and G.L. Kok, Correction to "Henry's law determinations for aqueous solutions of hydrogen peroxide, methylhydroperoxide, and peroxyacetic acid" by John A. Lind and Gregory L. Kok, *J. Geophys. Res.*, *99*, 21119, 1994.
- Lind, J.A., A.L. Lazrus, and G.L. Kok, Henry's law determinations for aqueous solutions of hydrogen peroxide, methylhydroperoxide, and peroxyacetic acid, *J. Geophys. Res.*, *91*, 7889-7895, 1986.
- Lind, J.A., A.L. Lazrus, and G.L. Kok, Aqueous phase oxidation of sulfur(IV) by hydrogen peroxide, methylhydroperoxide and peracetic acid, *J. Geophys. Res.*, *92*, 4171-4177, 1987.
- Madronich, S.A., and J.G. Calvert, Permutation reactions of organic peroxy radicals in the atmosphere, *J. Geophys. Res.*, *95*, 5697-5715, 1990.
- Marklund, S., The simultaneous determination of bis(hydroxymethylperoxide) (BHMP), hydroxymethylhydroperoxide (HMP) and  $\text{H}_2\text{O}_2$  with titanium (IV). Equilibria between the peroxides and the stabilities of HMP and BHMP at physiological conditions, *Acta Chem. Scand.*, *25*, 3517-3531, 1971.
- Merrill, J.T., and J.L. Moody, Synoptic meteorology and transport during the North Atlantic Regional Experiment (NARE) intensive, *J. Geophys. Res.*, *this issue*.
- Mohnen, V.A., and J.A. Kadlec, Cloud chemistry research at Whiteface mountain, *Tellus*, *41B*, 79-91, 1989.
- Penkett, S.A., B.M.R. Jones, K.A. Brice, and A.E. Eggleton, The importance of atmospheric  $\text{O}_3$  and  $\text{H}_2\text{O}_2$  in oxidizing  $\text{SO}_2$  in cloud and rainwater, *Atmos. Environ.*, *13*, 123-137, 1979.
- Sakugawa, H., I.R. Kaplan, W. Tsai, and Y. Cohen, Atmospheric hydrogen peroxide, *Environ. Sci. Technol.*, *24*, 1452-1462, 1990.
- Shankar, J., K.V.S.R. Rao, and L.V. Shastri, Peroxide formation in the gamma radiolysis of aerated aqueous solutions of methyl iodide, *J. Phys. Chem.*, *73*, 52-57, 1969.
- Sillman, S., The use of  $\text{NO}_x$ ,  $\text{HCHO}$ ,  $\text{H}_2\text{O}_2$  and  $\text{HNO}_3$  as empirical indicators for ozone- $\text{NO}_x$ -ROG sensitivity in urban locations, *J. Geophys. Res.*, *100*, 14175-14188, 1995.
- Simonaitis, R., K.J. Olszyna, and J.F. Meagher, Production of hydrogen peroxide and organic peroxides in the gas phase reactions of ozone with natural alkenes, *Geophys. Res. Lett.*, *18*, 9-12, 1991.
- Tremmel, H.G., W. Junkermann, F. Slemr, and U. Platt, On the distribution of hydrogen peroxide in the lower troposphere over the northeastern United States during late summer 1988, *J. Geophys. Res.*, *98*, 1083-1099, 1993.

P. H. Daum, L. I. Kleinman, J. H. Lee, and L. J. Nunnermacker, Brookhaven National Laboratory, Department of Applied Science, Environmental Chemistry Division, Upton, NY 11973-5000 (e-mail: phdaum@bnlux1.bnl.gov; kleinman@bnlcl6.bnl.gov; lindan@bnl.gov)

J. B. Weinstein-Lloyd, Chemistry and Physics Department, SUNY/Old Westbury, Old Westbury, NY 11568-0210 (e-mail: jlloyd@bnl.gov)

(Received May 10, 1995; revised October 17, 1995, accepted October 17, 1995.)